Acta Cryst. (1978). B34, 1051–1059

Structure Determination of Complex Oxides from X-ray Powder Patterns by the Method of Concentration Waves (Superstructures Based on the Fluorite Lattice)

BY B. I. POKROVSKII AND E. V. ISAEVA

Department of Chemistry, Moscow State University, Moscow 117234, *USSR*

(*Received* 15 *December* 1976; *accepted* 8 *July* 1977)

The structures of the complex oxides Sc_2O_3, $Ln_2M_2O_7$, $Sc_4Ti_3O_{12}$, Sc_2VO_5 and $Sc_9Ti_{10}O_{31\cdot2}$, which exemplify various types of superstructures based on the fluorite lattice, are discussed. The arrangement of the metal and O atoms and O vacancies over the sites of the basis fluorite matrix is determined from the X-ray powder photographs with a fundamentally new approach to the structure analysis, the concentration-wave method, which provides a means of solving the problem from the observed sets of superstructure reflections, without recourse to their intensities. The results obtained illustrate the potential of the concentration-wave method as applied to interpretation of structures of solids of widely varying chemical composition.

Solid solutions having fluorite (CaF_2) type structures frequently occur in systems comprising rare-earth metal oxides and oxides of Group IV and V elements. These phases are, as a rule, O deficient and contain O vacancies randomly distributed over the sites of the anionic sublattice. Their composition can be written $(M',M'')O_{2-x}\square_x$ where M' and M'' are two sorts of metal ions and $\square$ stands for O vacancies.

Lowering of temperature results in ordering of the arrangement of metal and O atoms and vacancies: a phase transition of the order–disorder type occurs, which manifests itself by the appearance of additional superstructure reflections in the X-ray diffraction pattern. The principal difficulty one encounters in interpreting structures of ordered phases formed from solid solutions arises from the scarcity of available structural information, which is mostly limited to powder photographs.

The shortcomings of the powder technique as applied to the solution of superstructures can, however, be overcome to a considerable extent by using the concentration-wave approach. This method makes it feasible to deduce the distribution of atoms from the observed set of superstructure reflections (in certain cases it furnishes a number of possible distribution variants) and obviates the need to analyse the reflection intensities, which are only included at the stage of refinement of the structure parameters.

Theory of the method

The essence of the concentration-wave method developed by Khachaturyan (1973) is as follows. The ordered arrangement of atoms of various sorts over the lattice sites is described by the distribution function $n(\mathbf{R})$ given as the superposition of plane concentration waves generated by the system of wave vectors related to the superstructure reflections.

$$n(\mathbf{R}) = c + \tfrac{1}{2}\sum_j [Q(\mathbf{K}_{j_s}) \exp(i\mathbf{K}_{j_s}\mathbf{R}) + Q(\mathbf{K}_{j_s}) \exp(-i\mathbf{K}_{j_s}\mathbf{R})]. \quad (1)$$

The wave vectors $\mathbf{K}_{j_s}$ of static waves $\exp(i\mathbf{K}_{j_s}\mathbf{R})$ are 2π times the superstructure vectors of the reciprocal lattice which belong to the first Brillouin zone of a disordered solid solution. Superstructure vectors related by symmetry operations of the substructure reciprocal lattice make up stars (the numbering of the stars is given by scripts s). Symbol c stands for the total concentration of atoms whose arrangement is described by the distribution function $n(\mathbf{R})$.

The amplitude of the static wave, $Q(\mathbf{K}_{j_s})$, represents the product of the long-range-order parameter η_s, having the same value for all wave vectors of a given star, and the coefficients $\gamma_s(j_s)$. The fully ordered arrangement is characterized by η_s equal to unity. The relations between the $\gamma_s(j_s)$ coefficients determine the symmetry of the distribution function with respect to reflections and rotations. (1) can be re-written in the form

$$n(\mathbf{R}) = c + \sum_s \eta_s \varepsilon_s(\mathbf{R}) \quad (2)$$

where symmetry-related terms are grouped together, and ε_s is

$$\varepsilon_s(\mathbf{R}) = \tfrac{1}{2}\sum_{j_s} [\gamma_s(j_s) \exp(i\mathbf{K}_{j_s}\mathbf{R}) + \gamma_s^*(j_s) \exp(-i\mathbf{K}_{j_s}\mathbf{R})]. \quad (3)$$

The distribution function $n(\mathbf{R})$ constructed from superstructure vectors should meet the following principal requirement: the number of different values it takes on the full set of basis lattice sites should be

greater by one than the number of long-range order parameters or, in other words, the number of stars included in (3).

Among superstructure vectors, there are low-symmetry irreducible ones, which cannot be decomposed into component vectors belonging to other stars of the first Brillouin zone. The vectors that can be obtained from the irreducible components are further referred to as reducible or derivative vectors.

The distribution function $n(\mathbf{R})$ first of all includes irreducible-vector static waves. If the distribution function with an irreducible basis takes more different values than the number of stars plus one, the basis should be extended by inclusion of reducible-vector waves.

The number of $n(\mathbf{R})$ and $\varepsilon_s(\mathbf{R})$ values is a function of the coefficients $\gamma_s(j_s)$. According to Kachaturyan (1973), nonzero $\gamma_s(j_s)$ values permissible for the sth star are given by

$$\gamma_s(j_s) = |\gamma_s| \exp[i\psi_s(j)] \tag{4}$$

where $|\gamma_s|$ has the same value for all vectors of a star and ψ_s stands for the ratio $\pi l_s/m$ [m is the least integer factor that transforms all vectors of a star, $(1/2\pi)\,\mathbf{K}_{j_s}$, into structure vectors of the reciprocal lattice $\mathbf{H}$, and l runs over the series of values: 0, 1, 2,..., $(2m-1)$].

The complex fluorite lattice comprises four interpenetrating f.c.c. Bravais lattices of parameter a.

The basic feature of the structure is the f.c.c. sublattice fully occupied by metal ions. The octahedral interstices of this sublattice make up another f.c.c. sublattice displaced from the basic one by the vector

$$\mathbf{h}^{\mathrm{oct}} = \left(\frac{aaa}{222}\right).$$

The tetrahedral interstices give the remaining two f.c.c. sublattices with the displacement vectors

$$\mathbf{h}_1^{\mathrm{tetr}} = \left(\frac{aaa}{444}\right) \quad \text{and} \quad \mathbf{h}_2^{\mathrm{tetr}} = \left(\frac{aaa}{444}\right).$$

In structures of the fluorite type, the latter two sublattices are occupied by anions. The octahedral interstices remain vacant or, in other words, are occupied by structure vacancies.

The solution of ordered structures does not necessarily require the construction of a general distribution function for the fluorite lattice as a whole. The task may be reduced to the determination of the distribution functions for each of the simple f.c.c. Bravais sublattices p ($p = 1, 2,\ldots$). It is clear from physical considerations that all four distribution functions should have the same translational symmetry, which is determined by the set of stars of low-symmetry vectors. Accordingly, all the atomic distribution functions $n(\mathbf{R})$ should have the same wave-vector basis. Despite having the same translational symmetry, the atomic distribution functions may differ in their behaviour with respect to rotations and reflections. Generally, the functions $n(p,\mathbf{R})$ should either be equal to each other or differ in parameters $c(p)$ and $\gamma_s(j_s,p)$ (Kachaturyan, 1973).

In principle, metal-ion distribution may have a higher symmetry than the distribution functions describing the arrangement of the O atoms and vacancies in the tetrahedral sublattices. In fact, negatively charged anions generate an electric field, the overall symmetry of which is determined by the symmetries of the electric fields of the two anionic sublattices. As the latter are equally displaced from the cationic sublattice, the resultant potential on the cationic sites may prove to be of higher symmetry than the component fields. On the other hand, the atomic distribution and potential-modulation functions should have the same form. It thus appears that the arrangement of metal ions may feature a higher symmetry compared with the arrangement of anions. This reduces the number of stars of superstructure vectors for the cationic sublattice but does not affect the translational symmetry of the structure as a whole, which is determined by the full set of low-symmetry vectors. Apart from that, the above-formulated rule of the number of distribution-function values remains valid for all sublattices.

Structure-factor moduli determining structure and superstructure reflection intensities in the absence of static or thermal displacements are given by

$$F_c(2\pi\mathbf{H}) = \Big|\sum_\alpha f_\alpha \sum_p c_\alpha(p) \exp(-i2\pi\mathbf{H}\mathbf{h}_p)\Big| \tag{5}$$

$$F_{cc}(2\pi\mathbf{H} + \mathbf{K}_{j_s}) = \Big|\sum_\alpha f_\alpha \sum_p \gamma_s(j,p) \exp[-i(2\pi\mathbf{H} + \mathbf{K}_{j_s})\mathbf{h}_p]\Big| \tag{6}$$

where f_α is the atomic scattering factor for atoms of type α.

In this work we apply the concentration-wave method to five solids exemplifying various types of superstructures based on the fluorite lattice. Three compounds of the series, Sc_2O_3, pyrochlore, $Sc_4Ti_3O_{12}$, have already been studied in detail by single-crystal X-ray diffraction; their structures are well known (Knop, Brisse, Castelliz & Sutarno, 1965; Náray-Szabó, 1969; Thornber, Bevan & Graham, 1968). Re-investigation of these solids has been undertaken in order to demonstrate the utility of the concentration-wave method in the interpretation of structures of phases of widely varying compositions. Two other compounds, Sc_2VO_5 and $Sc_9Ti_{10}O_{31.2}$, have not been subjected to structure analysis thus far; the structural data on these compounds are reported for the first time.

Structure of Sc_2O_3

Oxides of rare-earth metals and scandium (the so-called *C*-type rare-earth metal oxides) (Swanson, Fuyat & Ugrinic, 1954) belong to the first type of ordered phase derivative from fluorite that we are going to discuss. For example, consider the structure of Sc_2O_3. Its b.c.c. unit cell has twice the dimension of the fluorite cell. The cationic sublattice in Sc_2O_3 is fully occupied with atoms of one sort, whereas a quarter of the sites on the O sublattice are vacant. All the superstructure reflections are due to ordering in the arrangement of O atoms and structure vacancies. Hence, solution of the superstructure is given by a function $n(p,\mathbf{R})$ describing the distribution of vacancies (O atoms) over the sites of the anionic sublattices.

The construction of the $n(p,\mathbf{R})$ function first requires the determination of the wave vectors $\mathbf{q} = \mathbf{K}_j + 2\pi\mathbf{H}$ in the reciprocal-lattice space of a fluorite solid solution. In order to do this, we must write the coordinates of sites $\mathbf{h} = (h,k,l)$ of the reciprocal lattice of Sc_2O_3 in terms of the fluorite reciprocal-lattice basis, using the transformation matrix B:

$$\mathbf{q} = 2\pi\mathbf{B}\mathbf{h} = 2\pi \begin{pmatrix} \frac{1}{2} & 0 & 0 \\ 0 & \frac{1}{2} & 0 \\ 0 & 0 & \frac{1}{2} \end{pmatrix}_{Sc_2O_3} \begin{pmatrix} h \\ k \\ l \end{pmatrix}.$$

B is a reciprocal of the matrix that transforms the fluorite lattice basis to the basis of an ordered phase (Sc_2O_3 in the present case). Next, the distances between each of the superstructure reflections and the nearest structure reflection are calculated. The values thus obtained furnish the set of superstructure vectors $(1/2\pi)\,\mathbf{K}_{j_s}$ contained in the first Brillouin zone.

Each reflection in the powder photograph corresponds to a set of planes (*hkl*) with the same interplanar spacing. For that reason, each reflection corresponds not to a single vector $\mathbf{K}_{j_s}$ but to a set of superstructure vectors making up a star.

Table 1. *Parameters of the powder pattern of* Sc_2O_3

No.	*I*	*d* (Å)	*h k l*	$\mathbf{K}_s$
1	1·5	3·99	2 1 1	$\frac{1}{2}\frac{1}{2}0$
2	0·5	3·49	2 2 0	100
3	10	2·830	2 2 2	Structure
4	1	2·605	3 2 1	$\frac{1}{2}\frac{1}{2}0$
5	2	2·451	4 0 0	Structure
6	1	2·305	4 1 1	$\frac{1}{2}\frac{1}{2}0$
7	0·7	2·192	4 2 0	100
8	3·5	2·089	3 2 2	$\frac{1}{2}\frac{1}{2}0$
9	0·8	2·001	4 2 2	100
10	3	1·920	431, 510	$\frac{1}{2}\frac{1}{2}0$
11	1	1·791	5 2 1	$\frac{1}{2}\frac{1}{2}0$
12	10	1·734	4 4 0	Structure
13	1	1·683	535, 433	$\frac{1}{2}\frac{1}{2}0$
14	0·7	1·630	422, 600	100
15	2	1·589	532, 611	$\frac{1}{2}\frac{1}{2}0$
16	1	1·550	6 2 0	100
17	2	1·513	5 4 1	$\frac{1}{2}\frac{1}{2}0$
18	7·5	1·478	6 2 2	Structure

Table 1 includes interplanar spacings obtained from the powder pattern of Sc_2O_3 and, for each reflection, indices *hkl* and the corresponding star of superstructure vectors. The coordinates of wave vectors are given in the basis $2\pi\mathbf{a}_1^*$, $2\pi\mathbf{a}_2^*$, $2\pi\mathbf{a}_3^*$ where $\mathbf{a}_1^*$, $\mathbf{a}_2^*$, and $\mathbf{a}_3^*$ are the mutually orthogonal basis vectors of the reciprocal lattice ($|\mathbf{a}_1^*| = |\mathbf{a}_2^*| = |\mathbf{a}_3^*| = 1/a$ where a is the f.c.c. fluorite lattice parameter).

As follows from Table 1, the superstructure of Sc_2O_3 is generated by two stars of superstructure vectors. Star $\mathbf{K}_1$ includes low-symmetry vectors

$$\mathbf{K}_1 = \{(\tfrac{1}{2}\tfrac{1}{2}0), (\tfrac{1}{2}\bar{\tfrac{1}{2}}0), (\tfrac{1}{2}0\tfrac{1}{2}), (\bar{\tfrac{1}{2}}0\tfrac{1}{2}), (0\tfrac{1}{2}\tfrac{1}{2}), (0\tfrac{1}{2}\bar{\tfrac{1}{2}}), (0\bar{\tfrac{1}{2}}\tfrac{1}{2}), (\bar{\tfrac{1}{2}}\bar{\tfrac{1}{2}}0), (\bar{\tfrac{1}{2}}0\bar{\tfrac{1}{2}}), (\tfrac{1}{2}0\bar{\tfrac{1}{2}}), (0\bar{\tfrac{1}{2}}\bar{\tfrac{1}{2}}), (0\bar{\tfrac{1}{2}}\tfrac{1}{2})\}.$$

The vectors of the second star, $\mathbf{K}_2$ {(100), (010), (001)}, represent the second harmonics of the vectors of star $\mathbf{K}_1$.

The $\varepsilon_2(\mathbf{R})$ function of the vectors of star $\mathbf{K}_1$ takes a form convenient for practical purposes, after a rather simple transformation of the scalar product $\mathbf{K}_{j_s}\mathbf{R}$ in (3), by writing it in the f.c.c. lattice coordinates. In fact, the radius vector of the f.c.c. lattice is given by: $\mathbf{R} = x\mathbf{a}_1 + y\mathbf{a}_2 + z\mathbf{a}_3$. Then, as the basis vectors of the orthogonal and reciprocal lattices are related by $(\mathbf{a}_i.\mathbf{a}_i^*) = 1$ and $(\mathbf{a}_j.\mathbf{a}_i^*) = 0$, the expression for $\varepsilon_1(\mathbf{R})$ becomes

$$\begin{aligned}\varepsilon_1(\mathbf{R}) = \varepsilon_1(x,y,z) = \gamma_1\{&\exp[i\psi(1)]\exp[i\pi(x+y)] \\ &+ \exp[i\psi(2)]\exp[i\pi(x-y)] \\ &+ \exp[i\psi(3)]\exp[i\pi(x+z)] \\ &+ \exp[i\psi(4)]\exp[i\pi(-x+z)] \\ &+ \exp[i\psi(5)]\exp[i\pi(y+z)] \\ &+ \exp[i\psi(6)]\exp[i\pi(y-z)] \\ &+ \text{complex conjugate}\}. \end{aligned} \quad (7)$$

The number of different values taken by (7) in running over the sites of the f.c.c. lattice depends on the phases $\psi(j)$.

For star $\mathbf{K}_1$, $m = 2$, and each of the $\psi_1(j)$ phases may thus have one of the four values: 0, $\pi/2$, π, and $3\pi/2$.

We may now construct two distribution functions $n(\mathbf{R}) = c + \eta_1\varepsilon_1(\mathbf{R})$:

$$\begin{aligned} n_1(\mathbf{R}) = c + 2\eta_1\gamma_1[&\cos\pi(x+y) + \sin\pi(x-y) \\ &+ \cos\pi(x+z) + \sin\pi(-x+z) \\ &+ \cos\pi(y+z) + \sin\pi(y-z)] \end{aligned} \quad (8)$$

$$\begin{aligned} n_2(\mathbf{R}) = c + 2\eta_1\gamma_1[&\cos\pi(x+y) - \sin\pi(x-y) \\ &+ \cos\pi(x+z) - \sin\pi(-x+z) \\ &+ \cos\pi(y+z) - \sin\pi(y-z)] \end{aligned} \quad (9)$$

both of which meet the requirement cited in the theoretical introduction, *i.e.* to take on a value which is more by one than the number of long-range order parameters, and may therefore correspond to some ordered atomic arrangement.

We have for (8) $\psi(1) = \psi(3) = \psi(5) = 0$, $\psi(2) = \psi(4) = \psi(6) = \pi/2$, and for (9) $\psi(1) = \psi(3) = \psi(5) = 0$, $\psi(2) = \psi(4) = \psi(6) = 3\pi/2$.

By definition, the function that describes the distribution of atoms (vacancies) in a fully ordered solid of a stoichiometric composition may be equal to either zero or unity. When applied to (8) and (9), this condition yields

$$n_1 = c + 6\eta_1\gamma_1 = 1,$$
$$n_2 = c - 2\eta_1\gamma_1 = 0. \qquad (10)$$

Solution of this system gives the stoichiometric composition c_{st} of $\frac{1}{4}$ and the product $\eta_1\gamma_1$ value of $\frac{1}{8}$ for each of the f.c.c. Bravais sublattices.

The result obtained predicts an even distribution of vacancies between two tetrahedral sublattices.

In principle, distributions (8) and (9) describe crystallographically equivalent superstructures, and either of the two can be used to describe the arrangement of vacancies over the sites of a given sublattice. The overall symmetry of the anionic network, however, depends on the mutual arrangement of vacancies in two tetrahedral sublattices and hence on the relation between the respective distribution functions. It is reasonable to assume that, among the possible crystal structures corresponding to various combinations of the distribution functions, the actual structure has the lowest lattice energy. For our purposes we may regard metal oxide phases as pseudo-ionic crystals whose internal energy is mainly determined by Coulomb terms. The latter reduce to a minimum when vacancies positioned nearest to the metal atom (in the first coordination sphere) are separated furthest from each other.

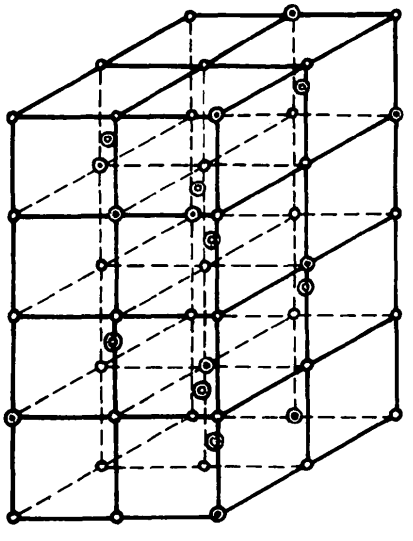

Fig. 1. A fragment of the structure of Sc_2O_3. ○ Oxygen atom, ⊙ oxygen vacancy, ◎ scandium atom.

Each positively charged metal ion in the fluorite lattice has eight nearest-neighbour anion sites, which form a cube with half the dimension of the f.c.c. unit cell. It is clear that, in terms of the electrostatic model, the arrangement with vacancies located on a body diagonal of this cube is energetically favoured over that with a face-diagonal separation between vacancies. Still less favourable are structures in which vacancies occupy adjacent vertices. The latter situation occurs when the same distribution function fits both anionic sublattices. On the other hand, the use of (8) for one and (9) for the other sublattice yields an energetically favourable arrangement. This combination corresponds to the structure in which Sc atoms occupying vertices of the f.c.c. unit cell are surrounded by six O atoms and two vacancies located at the ends of a body diagonal. The remaining Sc ions have a similar environment, but with vacancies occupying opposite corners of one of the cube faces. The mutual arrangement of O atoms and vacancies is shown in Fig. 1 where the principal fragment of the Sc_2O_3 unit cell is depicted.

O vacancies may be treated as tetrahedral interstices in the metal lattice. It follows from the theory of static distortions (Krivoglaz & Tikhonova, 1960) that interstitial atoms displace matrix atoms from the sites of an 'average' lattice while retaining their own positions. Such displacements may generate 'superposition' reflections, which correspond to combinations of two or more independent vectors entering function $n(\mathbf{R})$.

This in particular is the reason why powder photographs of Sc_2O_3 contain weak reflections generated by star $\mathbf{K}_2$, which does not appear in the expression for $n(\mathbf{R})$. These reflections originate from displacements of Sc atoms from the sites of the matrix fluorite lattice. Their intensities are low and increase with $\mathbf{q}$, in agreement with what may be expected for reflections resulting from atomic displacements.

To conclude the discussion of the Sc_2O_3 structure, we should note that during the analysis, a number of alternative structure variants have been considered and ruled out, that for one reason or another could not have been fitted to the functions $n(\mathbf{R}, p)$ constructed from the superstructure vectors of the Sc_2O_3 lattice. Thus, the distribution of all vacancies over the sites of one of the sublattices with concentration c equal to $\frac{1}{2}$ has to be excluded because no distribution function with a stoichiometric concentration of $\frac{1}{2}$ can be written with the superstructure vector basis defined as described above. Because of space limitations we cannot consider the finer details of structure analysis; therefore only the principal points will be discussed.

Pyrochlore-type structures

Ordered phases of the composition $Ln_2M_2O_7$ are frequently referred to as pyrochlores, which reflects the fact that they are isostructural with the mineral having the same name, $NaCaNbTaO_6F$ (Knop *et al.*, 1965). The structure of pyrochlore may also be regarded as a derivative of fluorite and formed by ordering of the arrangement of metal and O atoms over the sites of the fluorite lattice. The f.c.c. lattice of pyrochlore has twice the parameter of fluorite. The metal sublattice contains equal numbers of rare-earth metal atoms (Ln) and Group IV metal atoms (M), where M stands for Ti, Zr, Hf. One eighth of the sites on two tetrahedral anionic sublattices are vacant; the remaining sites are occupied by O.

The superstructure reflections give two stars:

$$\mathbf{K}_2 = \{(100), (010), (001)\}$$
$$\mathbf{K}_3 = \{(\tfrac{1}{2}\tfrac{1}{2}\tfrac{1}{2}), (\bar{\tfrac{1}{2}}\tfrac{1}{2}\tfrac{1}{2}), (\tfrac{1}{2}\bar{\tfrac{1}{2}}\tfrac{1}{2}), (\tfrac{1}{2}\tfrac{1}{2}\bar{\tfrac{1}{2}})\}.$$

This basis generates a single $n(\mathbf{R})$ function

$$\begin{aligned} n(\mathbf{R}) = c &+ \eta_2\gamma_2[\exp(i2\pi x) + \exp(i2\pi y) + \exp(i2\pi z)] \\ &+ \eta_3\gamma_3\{\exp[i\pi(x+y+z)] \\ &+ \exp[i\pi(-x+y+z)] + \exp[i\pi(x-y+z)] \\ &+ \exp[i\pi(x+y-z)]\} \end{aligned} \tag{11}$$

which takes three different values in most f.c.c. Bravais lattice sites:

$$n_1 = c + 3\eta_2\gamma_2 + 4\eta_3\gamma_3$$
$$n_2 = c + 3\eta_2\gamma_2 - 4\eta_3\gamma_3$$
$$n_3 = c - \eta_2\gamma_2.$$

Setting $n_1 = 1$ and $n_2 = n_3 = 0$, we have $c_{st} = \frac{1}{8}$, $\eta_2\gamma_2 = \frac{1}{2}$, and $\eta_3\gamma_3 = \frac{1}{8}$.

The value of $\frac{1}{8}$ for the stoichiometric concentration indicates that equal numbers of vacancies occur in both tetrahedral sublattices.

Such a distribution of O atoms and vacancies results in that only star $\mathbf{K}_3$ enters the potential modulation function, $\varphi(\mathbf{R})$, for the metal sublattice, and the distribution of metal atoms is given by:

$$\begin{aligned} n(\mathbf{R}) = c &+ \eta_3\gamma_3\{-\exp[i\pi(x+y+z)] \\ &+ \exp[i\pi(-x+y+z)] + \exp[i\pi(x-y+z)] \\ &+ \exp[i\pi(x+y-z)]\}. \end{aligned} \tag{12}$$

Function (12) takes on two values:

$$n_1 = c + 2\eta_3\gamma_3$$
$$n_2 = c - 2\eta_3\gamma_3.$$

With $n_1 = 1$ and $n_2 = 0$, c_{st} is $\frac{1}{2}$ and $\eta_3\gamma_3$ is $\frac{1}{4}$.

The pyrochlore reflections with *hkl* indices all odd (the $\mathbf{K}_3$ vectors) are as a rule much stronger than those having even indices (the $\mathbf{K}_2$ vectors), which reflects the difference in the structures of the oxygen (11) and metal (12) distribution functions.

The stoichiometric concentration values for functions (12) and (11) coincide with the concentrations of metal atoms and vacancies, respectively, in $Ln_2M_2O_7$. The structural formula of the compounds that crystallize in the pyrochlore lattice can thus be written in the form

$$[Ln_{\frac{1}{2}}M_{\frac{1}{2}}][O_{\frac{7}{8}}\square_{\frac{1}{8}}][O_{\frac{7}{8}}\square_{\frac{1}{8}}] = Ln_2M_2O_7$$

where the atomic groups occupying the same sublattice are bracketed.

The mutual atomic arrangement in $Ln_2M_2O_7$ is shown in Fig. 2, where a quarter of the pyrochlore unit cell is depicted.

It now remains to determine what cations occupy each of the two sets of sites n_1 and n_2.

Crystallographically, the difference between the sites of the f.c.c. metal-ion sublattice corresponding to different values of function (12) in the fully ordered structure is the difference in coordination numbers. Sites n_1 have six O and two vacancy nearest neighbours, while ions located on sites n_2 are eight-coordinate.

The coordination number six is characteristic for tetravalent Ti, Zr, and Hf, while bulkier rare-earth cations are more likely to occur in eight-coordinate positions (Náray-Szabó, 1969). It thus appears reasonable to assume that sites n_1 are occupied by M and sites n_2 by Ln cations.

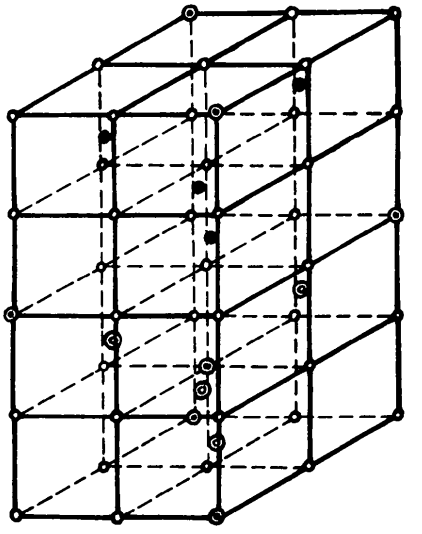

Fig. 2. A fragment of the structure of $Ln_2M_2O_7$. ○ Oxygen atom, ⊙ oxygen vacancy, ● Ln atom, ◎ M atom.

Structure of Sc_2VO_5

Compound Sc_2VO_5 occurs in the system Sc_2O_3–VO_2 (Mikhailov, Pokrovskii & Komissarova, 1971). Its X-ray powder pattern (both reflections corresponding to the basis fluorite structure and superstructure reflections) can be indexed in a tetragonal lattice with unit-cell dimensions $a' = a\sqrt{2} = 6{\cdot}954$, $c = 3a = 14{\cdot}372$ Å, where a is, as before, the basis fluorite cell parameter.

One third of the metal sublattice sites are occupied by V atoms. The remaining sites contain Sc. One sixth of the fluorite anionic sites are vacant. The indexing of the Sc_2VO_5 X-ray powder pattern given in Table 2 is taken from Mikhailov *et al.* (1971). For each superstructure reflection, the corresponding star of superstructure vectors belonging to the first Brillouin zone of the fluorite f.c.c. lattice has been determined. These data are also included in Table 2.

The ordering of the atomic arrangement in the structure of Sc_2VO_5 is governed by superstructure vectors making up stars:

$$\mathbf{K}_2 = \{(100), (010), (001)\}$$
$$\mathbf{K}_4 = \{(00\tfrac{2}{3}), (00\bar{\tfrac{2}{3}})\}$$
$$\mathbf{K}_5 = \{(\tfrac{1}{2}\tfrac{1}{2}0), (\tfrac{1}{2}\bar{\tfrac{1}{2}}0), (\bar{\tfrac{1}{2}}\bar{\tfrac{1}{2}}0), (\bar{\tfrac{1}{2}}\tfrac{1}{2}0)\}$$
$$\mathbf{K}_6 = \{(\tfrac{1}{2}\tfrac{1}{2}\tfrac{1}{3}), (\tfrac{1}{2}\tfrac{1}{2}\bar{\tfrac{1}{3}}), (\tfrac{1}{2}\bar{\tfrac{1}{2}}\tfrac{1}{3}), (\bar{\tfrac{1}{2}}\tfrac{1}{2}\tfrac{1}{3}),$$
$$(\bar{\tfrac{1}{2}}\bar{\tfrac{1}{2}}\tfrac{1}{3}), (\bar{\tfrac{1}{2}}\bar{\tfrac{1}{2}}\bar{\tfrac{1}{3}}), (\bar{\tfrac{1}{2}}\tfrac{1}{2}\bar{\tfrac{1}{3}}), (\tfrac{1}{2}\bar{\tfrac{1}{2}}\bar{\tfrac{1}{3}})\}$$
$$\mathbf{K}_7 = \{(10\tfrac{1}{3}), (10\bar{\tfrac{1}{3}}), (01\tfrac{1}{3}), (01\bar{\tfrac{1}{3}})\}.$$

Table 2. *Parameters of the powder pattern of* Sc_2VO_5

No.	I	d (Å)	$h\,k\,l$	$\mathbf{K}_s$
1	1	7·28	0 0 2	$00\frac{2}{3}$
2	1	4·11	1 1 2	$10\frac{2}{3}$
3	2	3·42	1 1 3	0 1 0
4	5	3·37	2 0 1	$00\frac{2}{3}$
5	1	3·03	2 1 1	$\frac{1}{2}\frac{1}{2}\frac{1}{3}$
6	100	2·826	2 0 3	Structure
7	4	2·458	2 2 0	Structure
8	3	2·431	0 0 6	Structure
9	1	2·327	2 2 2	$00\frac{2}{3}$
10	1	2·236	2 0 5	$00\frac{2}{3}$
11	3	2·196	2 2 3	0 0 1
12	4	2·038	2 2 4	$00\frac{2}{3}$
13	2	1·935	3 2 0	$\frac{1}{2}\frac{1}{2}0$
14	4	1·870	3 2 2	$\frac{1}{2}\frac{1}{2}\frac{1}{3}$
15	1	1·821	0 0 8	$00\frac{2}{3}$
16	1	1·785	2 0 7	$00\frac{2}{3}$
17	8	1·738	4 0 0	Structure
18	20	1·729	2 2 6	Structure
19	1	1·691	4 0 2	$00\frac{2}{3}$
20	1	1·636	4 0 3	0 0 1
21	1	1·582	1 0 9	$\frac{1}{2}\frac{1}{2}0$
22	1	1·546	4 2 1	$00\frac{2}{3}$
23	2	1·496	3 3 4	$00\frac{2}{3}$
24	10	1·481	4 2 3	Structure
25	7	1·468	2 0 9	Structure
26	2	1·436	2 1 9	$\frac{1}{2}\frac{1}{2}0$
27	2	1·414	4 0 6	Structure

The vectors belonging to stars $\mathbf{K}_4$ and $\mathbf{K}_5$ are irreducible; all the other vectors are derivatives from them.

For stars $\mathbf{K}_4$ and $\mathbf{K}_7$, not all vectors that can be obtained from symmetry consideration of the reciprocal fluorite lattice are included, because the $\gamma_s(j_s)$ coefficients for some of these vectors reduce to zero in tetragonal superstructures. Such vectors will not be considered here.

Four crystallographically equivalent distribution functions with different phases can be constructed:

$$n(\mathbf{R}) = c + \eta_4\varepsilon_4(\mathbf{R}) + \eta_5\varepsilon_5(\mathbf{R}) + \eta_6\varepsilon_6(\mathbf{R}) \quad (13)$$

that, first, take for the set of sites of the f.c.c. lattice values greater by one in number than the long-range order parameters and, second, fit the stoichiometry of the solid.

We will now apply (13) to superstructures of the compositions $c_{st} = \frac{1}{6}, \frac{1}{3}, \frac{1}{2}$. Four $n(\mathbf{R})$ values make up the system

$$n_1 = c + 2\eta_4\gamma_4 + 2\eta_5\gamma_5 + 4\eta_6\gamma_6$$
$$n_2 = c - \eta_4\gamma_4 + 2\eta_5\gamma_5 - 2\eta_6\gamma_6$$
$$n_3 = c + 2\eta_4\gamma_4 - 2\eta_5\gamma_5 - 4\eta_6\gamma_6$$
$$n_4 = c - \eta_4\gamma_4 - 2\eta_5\gamma_5 + 2\eta_6\gamma_6.$$

Solution of this system yields

$$c = \tfrac{1}{6}(n_1 + 2n_2 + n_3 + 2n_4)$$
$$\eta_4\gamma_4 = \tfrac{1}{6}(n_1 - n_2 + n_3 - n_4)$$
$$\eta_5\gamma_5 = \tfrac{1}{12}(n_1 + n_2 - n_3 + n_4)$$
$$\eta_6\gamma_6 = \tfrac{1}{12}(n_1 - n_2 - n_3 - n_4).$$

The arrangement of the O atoms over the superstructure sites that corresponds to the energy minimum (within the electrostatic model) is described by the following vacancy-distribution functions:

$$n(\mathbf{R}, 1) = \tfrac{1}{6} + \tfrac{1}{3}\cos\tfrac{4\pi z}{3} + \tfrac{1}{6}[\cos\pi(x+y) + \sin\pi(x-y)] + \tfrac{1}{6}[\cos\pi(x+y+\tfrac{2z}{3}) + \cos\pi(x+y-\tfrac{2z}{3}) + \sin\pi(x-y+\tfrac{2z}{3}) + \sin\pi(x-y-\tfrac{2z}{3})] \quad (14)$$

for one of the anionic sublattices and

$$n(\mathbf{R}, 2) = \tfrac{1}{6} + \tfrac{1}{3}\cos\tfrac{4\pi z}{3} + \tfrac{1}{6}[\cos\pi(x+y) - \sin\pi(x-y)] + \tfrac{1}{6}[\cos\pi(x+y+\tfrac{2z}{3}) + \cos\pi(x+y-\tfrac{2z}{3}) - \sin\pi(x-y+\tfrac{2z}{3}) - \sin\pi(x-y-\tfrac{2z}{3})] \quad (15)$$

for the other.

The $n(\mathbf{R})$ function describing the distribution of V atoms over crystal sites (fully ordered arrangement),

which is symmetry consistent with the overall arrangement of vacancies, only includes star $\mathbf{K}_4$ vectors:

$$n(\mathbf{R}) = \tfrac{1}{3} + \tfrac{2}{3}\cos\tfrac{4\pi z}{3} \qquad (16)$$

(that is, $c_{st} = \frac{1}{3}$ and $\eta_4\gamma_4 = \frac{1}{3}$). At elevated temperatures, partly disordered structures may occur with a different overall symmetry of vacancy arrangement. If the long-range-order parameters $\eta_5(p)$ and $\eta_6(p)$ in (14) and (15) have different temperature dependences, the general form of (13) should be used to describe the distribution of metal atoms. At temperatures well below the phase-transition point, the coefficients $\eta_5\gamma_5$ and $\eta_6\gamma_6$ approach zero.

Sc_2VO_5 has a layer structure (Fig. 3). Down the z axis, V layers alternate with pairs of Sc layers. The unit cell contains two V and four Sc layers. The V ions located on the basal plane have six O and two vacancy nearest neighbours. The latter belong to different tetrahedral sublattices and lie at the ends of a body diagonal of the coordination cube.

Sc atoms that make up the adjacent layer have a single vacancy nearest neighbour; their coordination polyhedra contain seven O atoms. The next metal-ion layer comprises Sc ions octahedrally coordinated with O (octahedra are formed by withdrawal of two O atoms with a face-diagonal separation between them from the original cube).

The fourth layer is occupied by V ions coordinated in a way similar to the Sc ions of the preceding layer. The principal difference is that half the metal ions have vacancies in the anionic layer that lies below the metal layer, while the other half have vacancies in the upper layer.

The fifth layer, occupied by Sc, repeats the third, and the sixth layer repeats the second.

O vacancies displace metal ions. The vacancies located on the top or bottom faces of anionic cubes should have the strongest action in displacing metals mainly along the c axis. As a result, reflections corresponding to derivative factors belonging to stars $\mathbf{K}_2$ and $\mathbf{K}_7$ appear. As expected, star $\mathbf{K}_2$ generates the stronger reflections. Comparison of the $\eta_s\gamma_s$ parameter values in distribution functions (14), (15) and (16) predicts the reflections from superstructure vectors of star $\mathbf{K}_4$ to be much stronger than those generated by stars $\mathbf{K}_5$ and $\mathbf{K}_6$. This prediction is again in excellent agreement with the observed intensity pattern (Table 2).

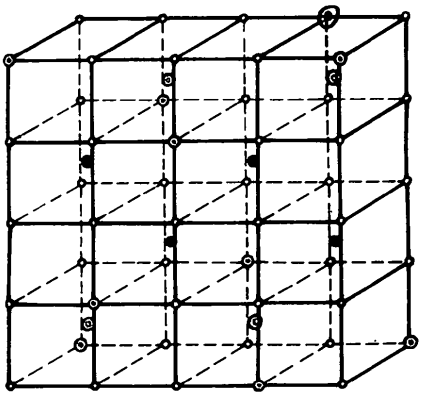

Fig. 3. A fragment of the structure of Sc_2VO_5. ○ Oxygen atom, ⊙ oxygen vacancy, ◎ vanadium atom, ● scandium atom.

Structure of the type $Sc_4Ti_3O_{12}$

We now proceed to examples of rhombohedrally distorted f.c.c. fluorite lattices.

Compound $Sc_4Ti_3O_{12}$, which occurs in the system Sc_2O_3–TiO_2, forms a disordered solid solution having the fluorite structure above 1170°C (Komissarova, Pokrovskii & Nechaeva, 1966). Crystals of the ordered phase are rhombohedral, the hexagonal unit-cell parameters are: $a' = a\sqrt{\frac{7}{2}} = 9{\cdot}094$, $c = a\sqrt{3} = 8{\cdot}535$ Å. The cell contains 21 metal atoms (12 Sc and 9 Ti). Of a total of 42 anionic sites per cell, 36 sites are occupied by O, and the remaining 6 (one seventh part) by structure vacancies. A single star of superstructure vectors generates all superstructure reflections observed in the powder photograph (Table 3):

$$\mathbf{K}_8 = \{(\tfrac{5}{7}\tfrac{3}{7}\bar{\tfrac{1}{7}}), (\bar{\tfrac{1}{7}}\tfrac{5}{7}\tfrac{3}{7}), (\tfrac{3}{7}\bar{\tfrac{1}{7}}\tfrac{5}{7}), (\tfrac{5}{7}\tfrac{3}{7}\bar{\tfrac{1}{7}}), (\bar{\tfrac{1}{7}}\tfrac{5}{7}\tfrac{3}{7}), (\tfrac{3}{7}\bar{\tfrac{1}{7}}\tfrac{5}{7})\}.$$

The distribution function

$$n(\mathbf{R}) = c + 2\eta_8\gamma_8[\cos\tfrac{2}{7}\pi(5x + 3y - z) + \cos\tfrac{2}{7}\pi(-x + 5y + 3z) + \cos\tfrac{2}{7}\pi(3x - y + 5z)] \qquad (17)$$

takes only two values in going over the sites of the f.c.c. lattice:

$$n_1 = c + 6\eta_8\gamma_8$$

$$n_2 = c - \eta_8\gamma_8.$$

With $n_1 = 1$ and $n_2 = 0$, we have $c_{st} = \frac{1}{7}$ and $\eta_8\gamma_8 = \frac{1}{7}$. This result is only compatible with one mode of

Table 3. *Parameters of the powder pattern of* $Sc_4Ti_3O_{12}$

No.	I	d (Å)	$hkil$	$\mathbf{K}_s$
1	6	4·54	11$\bar{2}$0	$\frac{5}{7}\frac{3}{7}\bar{\frac{1}{7}}$
2	10	3·74	01$\bar{1}$2	$\frac{5}{7}\frac{3}{7}\bar{\frac{1}{7}}$
3	8	3·57	02$\bar{2}$1	$\frac{5}{7}\frac{3}{7}\bar{\frac{1}{7}}$
4	35	2·841	0003	
5	100	2·802	21$\bar{3}$1	Structure
6	25	2·438	21$\bar{3}$2	Structure
7	8	2·406	11$\bar{2}$3	$\frac{5}{7}\frac{3}{7}\bar{\frac{1}{7}}$
8	7	2·265	22$\bar{4}$0	$\frac{5}{7}\frac{3}{7}\bar{\frac{1}{7}}$
9	3	2·110	13$\bar{4}$1	$\frac{5}{7}\frac{3}{7}\bar{\frac{1}{7}}$
10	12	2·057	10$\bar{1}$4	$\frac{5}{7}\frac{3}{7}\bar{\frac{1}{7}}$
11	12	1·925	30$\bar{3}$3	$\frac{5}{7}\frac{3}{7}\bar{\frac{1}{7}}$
12	5	1·871	02$\bar{2}$4	$\frac{5}{7}\frac{3}{7}\bar{\frac{1}{7}}$
13	40	1·730	21$\bar{3}$4	
14	35	1·715	14$\bar{5}$0	Structure

arrangement of O vacancies: vacancies are equally distributed between two tetrahedral sublattices over the positions generated by one and the same distribution function.

The metal atoms located on the threefold axis (one seventh of all metal atoms) have only six O nearest neighbours; vacancies occupy two corners of the anionic cube and have a body-diagonal separation between them. The rest of the metal atoms have one O vacancy in the first coordination sphere (Fig. 4).

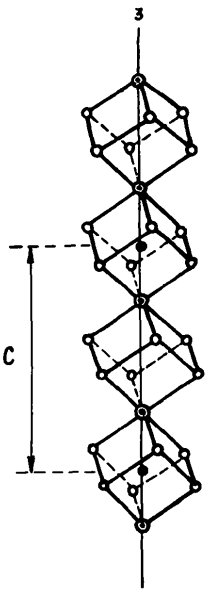

Fig. 4. Arrangement of atoms in $Sc_4Ti_3O_{12}$ seen in projection down the threefold axis. ○ Oxygen atom, ⊙ oxygen vacancy, ● metal atoms (Sc,Ti).

Table 4. *Parameters of the powder pattern of* $Sc_9Ti_{10}O_{31\cdot2}$

No.	I	d (Å)	$h\,k\,i\,l$	Star index s
1	1	4·24	1 2 $\bar{3}$ 1	9, 10
2	2	3·755	2 2 $\bar{4}$ 0	11
3	5	3·316	3 1 $\bar{4}$ 1	9, 10, 11
4	2	3·199	2 1 $\bar{3}$ 2	9, 10
5	100	2·812	2 3 $\bar{5}$ 1 0 0 $\bar{0}$ 3	Structure
6	10	2·434	2 3 $\bar{5}$ 2	Structure
7	2	2·356	1 4 $\bar{3}$ 2 3 0 $\bar{3}$ 3	9, 11 10
8	7	2·250	1 5 $\bar{6}$ 1 2 2 $\bar{4}$ 3	9, 10 11
9	2	2·122	2 4 $\bar{6}$ 2	9, 11
10	3	2·073	3 4 $\bar{7}$ 1	9, 10
11	1	1·996	1 4 $\bar{5}$ 3	9, 10
12	5	1·935	1 2 $\bar{3}$ 4	9, 11
13	4	1·818	3 1 $\bar{4}$ 4	9, 11
14	30	1·721	7 1 $\bar{8}$ 0 2 3 $\bar{5}$ 4	Structure
15	2	1·673	1 0 $\bar{1}$ 5 5 2 $\bar{7}$ 3	11 9, 10
16	1	1·637	3 6 $\bar{9}$ 0	9, 11
17	1	1·598	4 2 $\bar{6}$ 4	9, 10
18	2	1·563	1 5 $\bar{6}$ 4	9, 10

The stoichiometric concentration $c_{st} = \frac{1}{7}$ that appears in the distribution (17) differs considerably from the concentration of both Sc ($c_{Sc} = \frac{4}{7}$) and Ti ($c_{Ti} = \frac{3}{7}$). It appears from this that the occupation probabilities for a given site with respect to the two metals are approximately the same. The tendency of tetravalent Ti to form coordination octahedra with O (Náray-Szabó, 1969), however, favours the structure in which all octahedral sites and $\frac{1}{3}$ of the heptacoordinate positions are occupied by Ti, while Sc occupies the remaining $\frac{2}{3}$ positions with coordination number 7.

The structure described here for $Sc_4Ti_3O_{12}$ is analogous to that of $Sc_4Zr_3O_{12}$ determined earlier (Thornber *et al.*, 1968).

Structure of $Sc_9Ti_{10}O_{31\cdot2}$

The last compound we are going to discuss provides an example of an ordered phase whose stoichiometric composition is unknown beforehand. High-temperature (1400°C) sintering of a mixture of Sc and Ti oxides under hydrogen leads to the formation of a phase with a rather narrow region of homogeneity having the composition $(Sc,Ti)_{19}O_{31+\delta}$ where δ is near 0·2. The Ti valency state varies from (III) to (IV).

The X-ray powder pattern (Table 4) contains the basis fluorite and additional superstructure reflections that can be indexed in a rhombohedral lattice. The hexagonal unit cell has dimensions $a' = a\sqrt{\frac{19}{2}} = 15{\cdot}83$ and $c = a\sqrt{3} = 8{\cdot}416$ Å, $Z = 3$.

The superstructure reflections are generated by vectors of stars:

$$\mathbf{K}_9 = \{(\tfrac{\bar{10}}{19}\tfrac{6}{19}\tfrac{4}{19}), (\tfrac{4}{19}\tfrac{\bar{10}}{19}\tfrac{6}{19}), (\tfrac{6}{19}\tfrac{4}{19}\tfrac{\bar{10}}{19}), (\tfrac{10}{19}\tfrac{6}{19}\tfrac{\bar{4}}{19}), (\tfrac{\bar{4}}{19}\tfrac{10}{19}\tfrac{\bar{6}}{19}), (\tfrac{\bar{6}}{19}\tfrac{\bar{4}}{19}\tfrac{10}{19})\}$$

$$\mathbf{K}_{10} = \{(\tfrac{17}{19}\tfrac{5}{19}\tfrac{\bar{3}}{19}), (\tfrac{\bar{3}}{19}\tfrac{17}{19}\tfrac{5}{19}), (\tfrac{5}{19}\tfrac{\bar{3}}{19}\tfrac{17}{19}), (\tfrac{\bar{17}}{19}\tfrac{\bar{5}}{19}\tfrac{3}{19}), (\tfrac{3}{19}\tfrac{\bar{17}}{19}\tfrac{\bar{5}}{19}), (\tfrac{\bar{5}}{19}\tfrac{3}{19}\tfrac{\bar{17}}{19})\}$$

$$\mathbf{K}_{11} = \{(\tfrac{1}{19}\tfrac{7}{19}\tfrac{11}{19}), (\tfrac{11}{19}\tfrac{1}{19}\tfrac{7}{19}), (\tfrac{7}{19}\tfrac{11}{19}\tfrac{1}{19}), (\tfrac{\bar{1}}{19}\tfrac{7}{19}\tfrac{\bar{11}}{19}), (\tfrac{\bar{11}}{19}\tfrac{\bar{1}}{19}\tfrac{7}{19}), (\tfrac{7}{19}\tfrac{\bar{11}}{19}\tfrac{\bar{1}}{19})\}.$$

The distribution function has the form

$$\begin{aligned} n(x,y,z) = c &+ 2\eta_9\gamma_9[\cos\tfrac{2\pi}{19}(-10x + 6y + 4z) \\ &+ \cos\tfrac{2\pi}{19}(4x - 10y + 6z) \\ &+ \cos\tfrac{2\pi}{19}(6x + 4y - 10z)] \\ &+ 2\eta_{10}\gamma_{10}[\cos\tfrac{2\pi}{19}(17x + 5y - 3z) \\ &+ \cos\tfrac{2\pi}{19}(-3x + 17y + 5z) \\ &+ \cos\tfrac{2\pi}{19}(5x - 3y + 17z)] \\ &+ 2\eta_{11}\gamma_{11}[\cos\tfrac{2\pi}{19}(x + 7y + 11z) \\ &+ \cos\tfrac{2\pi}{19}(11x + y + 7z) \\ &+ \cos\tfrac{2\pi}{19}(7x + 11y + z)]. \end{aligned} \qquad (18)$$

Table 5. *Parameters of the distribution function* (18)

Variant	c_{st}	$\eta_9\gamma_9$	$\eta_{10}\gamma_{10}$	$\eta_{11}\gamma_{11}$
1	$\frac{1}{19}$	$\frac{1}{19}$	$\frac{1}{19}$	$\frac{1}{19}$
2	$\frac{6}{19}$	$-\frac{5}{76}$	$-\frac{5}{76}$	$\frac{5}{38}$
3	$\frac{6}{19}$	$-\frac{5}{38}$	$\frac{5}{38}$	$-\frac{9}{76}$
4	$\frac{6}{19}$	$\frac{5}{38}$	$-\frac{9}{76}$	$-\frac{5}{76}$

Function (18) takes four different values on the lattice sites (Table 5) and furnishes four variants of the ordered arrangement of vacancies in one of the sublattices comprising tetrahedral interstices. The parameters of the possible distributions are listed in Table 5.

With one of the O sublattices fully occupied, and the other having a vacancy concentration of $\frac{6}{19}$ (that is, O atoms occupy 13 of a total of 19 anionic sites), the stoichiometric composition is $(Sc,Ti)_{19}O_{32}$. Additional vacancies with a concentration of $\frac{1}{19}$ may be arranged according to variant 1 (Table 5). In this case, the stoichiometric composition is $(Sc,Ti)_{19}O_{31}$.

Experiment gives some 31·2 O atoms per unit cell, so that O atoms should occupy a certain proportion of the vacancy sites.

We may immediately rule out the variants that predict metals to have coordination numbers below 6. Still, there remain a number of alternative variants to be discussed. From a consideration of the intensities of the first several reflections, but without taking into account possible displacements of metal atoms, we arrive at the conclusion that variant 1 (Table 5) corresponds to the most probable vacancy distribution. Other distribution functions predict reflection intensities [see equations (5) and (6)] that differ significantly from those observed.

The c axis of the hexagonal unit cell coincides with the [111] direction in the fluorite f.c.c. cell. Along this direction, metal atoms form three closely packed layers alternating in the order *ABC ABC* ....

Metal atoms of layer *A* are surrounded by six O atoms and two vacancies, which occupy two corners of the anionic cube across a face diagonal.

The metal atoms of the next layer that lie on threefold axes have seven O nearest neighbours; the remaining atoms occupy alternating six- and seven-coordinate sites.

Metals in the third layer have only one vacancy in the first coordination sphere.

In going from the stoichiometric composition $(Sc,Ti)_{19}O_{31}$ to $(Sc,Ti)_{19}O_{31\cdot2}$, a proportion of vacancies are replaced with O atoms, which are randomly distributed over the vacancy sites.

Sc and Ti ions have closely similar crystallographic characteristics. Moreover, their atomic scattering factors are practically identical. For this reason, the distribution of Sc and Ti atoms over the metal sublattice sites can hardly be determined from X-ray diffraction. It may well be that additional superstructure occurs in the metal sublattice, which produces no observable effects. From general considerations, hexacoordinate sites should be occupied by Ti^{4+}, and heptacoordinate sites by Ti^{3+} and Sc^{3+}. It also seems probable that additional O atoms should arrange in such a way as to decrease the number of hexacoordinate sites with increase of the Ti^{3+} to Ti^{4+} ratio.

The authors are deeply indebted to A. G. Khachaturyan for valuable discussions.

References

KHACHATURYAN, A. G. (1973). *Phys. Status Solidi*, **60**, 9–37.

KNOP, O., BRISSE, F., CASTELLIZ, L. & SUTARNO (1965). *Can. J. Chem.* **43**, 2812–2826.

KOMISSAROVA, L. N., POKROVSKII, B. I. & NECHAEVA, V. V. (1966). *Dokl. Akad. Nauk SSSR*, **168**, 1076–1079.

KRIVOGLAZ, M. A. & TIKHONOVA, E. A. (1960). *Ukr. Fiz. Zh.* **5**, 158–173.

MIKHAILOV, YU. YA., POKROVSKII, B. I. & KOMISSAROVA, L. N. (1971). *Dokl. Akad. Nauk SSSR*, **198**, 344–346.

NÁRAY-SZABÓ, I. (1969). *Inorganic Crystal Chemistry*. Budapest: Akadémiai Kiadó.

SWANSON, H. E., FUYAT, R. K. & UGRINIC, G. M. (1954). *Natl Bur. Stand. US Circ.* 539, Vol. III, 27–28.

THORNBER, M. R., BEVAN, D. J. M. & GRAHAM, J. G. (1968). *Acta Cryst.* B**24**, 1183–1190.